Science of Sintering, **41** (2009) 309-317

doi: 10.2298/SOS0903309N

UDK 666.951:57.012.3

Influence of Diatomite Microstructure on its Adsorption Capacity for Pb(II)

S. Nenadovic[1a], M. Nenadovic[1b], R. Kovacevic[2], Lj. Matovic[1a], B. Matovic[1a], Z. Jovanovic[1c], J. Grbovic Novakovic[1*)]

[1]Vinca Institute of Nuclear Sciences, P.O.Box 522, 11 000 Belgrade, Serbia
[1a]Laboratory for Materials Sciences,
[1b]Laboratory for Atomic Physics,
[1c]Laboratory of Physics
[2]Institute for Mining and Metallurgy, Laboratory for ICP, Bor, Serbia

Abstract:

The effect of microstructural changes caused by mechanical modification on adsorption properties of diatomite samples were investigated. The microstructure has been characterized by X-ray diffraction (XRD), scanning electron microscopy (SEM) and atomic force microscopy (AFM) while the degree of metal adsorption was evaluated by Inductively Coupled Plasma Atomic Emission Spectrometry (ICP AES). The results show that metal sorption capacity of diatomite is considerably improved after mechanical modification and it can be attributed to amorphysation of the material. Immobilization efficiency increased from 22% for untreated to 81% for the treated sample after 5h at BPR 4.This qualifies natural diatomite as a material for wastewater remediation.

Keywords: *Waste water remediation, Diatomite, Microstrucructure, Ball milling, AFM*

1. Introduction

Diatomite ($SiO_2 \cdot nH_2O$) is pale-colored, soft, lightweight sedimentary rock composed principally of silica microfossils of aquatic unicellular algae. It is a highly porous structure, with good sorption ability, chemical inertness, low density and high surface area. Diatomite consists of a wide variety of shape and sized diatoms, typically from 10–200 μm, in a structure contains up to 80–90% voids [1]. The unique combination of physical and chemical properties of diatomite, make it applicable for the removal of heavy metals [2, 3] and organic pollutants [4] and as a filtration medium [5] in a number of industrial uses [1-7]. Taking into account its high permeability, high porosity and chemical inertness diatomite has been used as a cheap adsorbent for dyes removal [8]. Recently, the use of diatomite as a possible additive for improvement of hydrogen storage properties of MgH_2 has also been reported [9].

Contamination of ground and surface water with heavy metals is becoming a major concern since heavy metals like cadmium, chromium, lead are not biodegradable and tend to accumulate in living organisms causing various diseases and disorders. It is increasingly important to find a suitable medium for their adsorption. As an illustration, inhalation and

*) Corresponding author: jasnag@vinca.rs

ingestion of lead may cause various health diseases such as anemia, neuropsychological effects, liver diseases, gastrointestinal pathologies, terathogenic implications, even carcinogenesis [10, 11]. In addition, lead in soils may unfavorably affect soil ecology, agricultural production, or product and water quality [12]. In order to avoid such hazards, much effort has been made to enlarge remediation methods of lead contaminated soils. Chemical precipitation, membrane filtration, ion exchange, alum coagulation and activated carbon adsorption are some of the most commonly used methods for the treatment, and disposal, of metal-containing wastes [13-15]. Activated carbon adsorption is considered to be a particularly competitive and effective process for the removal of heavy metals at trace quantities [16]. However, the use of activated carbon is not suitable due to the high costs associated with production and regeneration of spent carbon [17]. The use of alternative low cost materials, natural ones, if possible, as potential sorbents for the removal of heavy metals has been highlighted nowadays [13, 18-25]. These cost-effective materials range from industrial by-products or waste, such as waste rubber tires [20], to agricultural products such as wool, rice straw, coconut husks and peat moss [21]. Other known natural materials like clay [22, 23], zeolites [23, 24] diatomite [25] have been investigated for their potential use as adsorbents for heavy metal.

In this work, local diatomaceous earth was tested as a potential sorbent for the removal of Pb(II) ions. Furthermore, the effect of surface modification of diatomite by ball milling on Pb(II) adsorption and on filtration quality was used to improve the sorption properties of natural diatomite. To our best knowledge this effect started to be considered very recently [18, 19] as a possible method for improvement of sorption properties. Anyhow, mechanically induced reactions have been successfully used for the degradation of organic pollutants such as hexachlorobenzene [26], hexabromobenzene [27] and more recently for the degradation of sulfonic acids [28].

2. Experimental part

Diatomite form Kolubara mine were processed by ball milling in a Turbula Type T2C Mixer mill operating at the standard milling frequency. Diatomite was mechanically treated for different time intervals (from 1 to 5 hours) in the air using ball to powder ratio (BPR) 4 [18].

The composition of diatomite was obtained using Inductively Coupled Plasma-Atomic Emission Spectrometry (ICP AES model Spectro CIROS vision, Kleve, Germany). ICP measurements were performed with the SPECTRO CIROSCCD ICP optical emission spectrometer with radial plasma viewing. The spectrometer in Paschen-Runge mounting consisted of a double-grating optical system with 22 CCD detectors. The spectral range between 125 nm and 770 nm is covered, allowing complete scans of the spectrum within 3s. All relevant ICP operating parameters are controlled by the software, such as gas flows and positioning of the torch (using stepper motors) in front of the patented optical plasma interface, allowing easy selection of the optimum operating conditions. Diatomite samples were contaminated at 25^{o}C with a solution of Pb(NO_3) pH=8.2 (99,99% Alfa Aesar) in concentration 2.95 mg/l. The flasks were sealed and shaken for 24 h, which was experimentally proved to be a sufficient time to reach equilibrium conditions [19]. Concentrations were calculated through the following mass balance:

$$q_{Pb(II)}^{24h} = \frac{\left(C_{Pb(II)}^{0} - C_{Pb(II)}^{24h}\right)}{W_{solid}} \cdot V_{liq} \qquad (1)$$

Where $q_{Pb(II)}^{24h}$ (mgkg^{-1}) is the Pb(II) concentration in the diatomite phase after 24 h of contact,

$C^{0}_{Pb(II)}$ and $C^{24h}_{Pb(II)}$ (mgl^{-1}) are the initial and equilibrium concentration of Pb(II) in the liquid phase, respectively, V_{liq} (l) in the volume of liquid solution and W_{solid} (kg) is the diatomite weight contacted with the diatomite. Immobilization efficiency, after each treatment interval, was calculated using following equation:

$$\eta(t)\% = \left(1 - \frac{C_{Pb(II)}(t)\cdot V_{leach}}{q^{24h}_{Pb(II)}\cdot W_{solid}}\right)\cdot 100 \qquad (2)$$

Where η(t) % is the immobilization efficiency (%) of the milling treatment for a time interval equal to t (s), C_{Pb} (mgl^{-1}) is the Pb (II) concentration in the sample, V_{leach} is leachate volume (l), $q^{24h}_{Pb(II)}$ ($mgkg^{-1}$) is the initial Pb (II) concentration in the untreated diatomite (cf. Eq. (1)) and W_{solid} (kg) is the diatomite weight undergone the test. From linear fit $\ln K_d = f\left(C^{24h}_{Pb(II)}\right)$ where K_d is distribution coefficient, calculated from the following equation:

$$K_d = \frac{\left(C^{0}_{Pb(II)} - C^{24h}_{Pb(II)}\right)}{C^{24h}_{Pb(II)}}\cdot\frac{V_{ilq}}{W_{solid}} \qquad (3)$$

one can obtain the value $\ln K^0$ (see Fig. 8) and thermodynamic parameters for Pb(II) sorption onto diatomite.

Microstructure and morphology of materials were recorded by X-ray diffraction analysis (XRD), scanning electron microscopy (SEM) using JEOL JSM 6460LV and Oxford Instrument INCA-X-sight at 25kV and atomic force microscopy AFM. The crystallite structure of diatomite before and after mechanical milling was examined by a X-ray diffractometer Siemens D-500, with Cu K_α Ni filtrated radiation. The diffracted X-rays were collected over 2θ range 20-80^o using a step width of 0.02^o and measuring for 1s per step.

The AFM studies were carried out on a Veeco MultiMode Quadrex IIIe in the tapping mode. Cantilever type is standard RTESP-Veeco production. Tip material is 0.5-2 Ωcm phosphorus (n) doped Si. AFM imaging was performed in tapping mode with a 15-20 μm high pyramidal tip. The resonance frequency of tip was 268.2 kHz. The scan rate was maintained in order of 2 Hz to get the optimal image quality. During the tapping mode it was very important to avoid thermal drift. The surface area was measured using Automatic surface area analyzer 4200, Leeds and Northrup Instruments.

3. Results and discussion

The chemical composition of the diatomite is as follows 79.72% SiO_2, 10.20% Al_2O_3. There are also water molecules and impurities consisting of $CaCO_3$, Fe_2O_3, TiO_2 .

The X ray pattern of untreated and 5 hours milled diatomite presented in Fig. 1 revealed that the raw diatomite and milled one are composed of three crystalline phases; SiO_2 (quartz form) and $CaCO_3$ in the calcite and dolomite forms (confirming chemical analysis) and some Al_2O_3. This indicates that there are no reactions between soil compounds or phase transformations during the mechanical milling. The obvious effect is a partial amorphization of SiO_2 phases upon mechanical treatment definite by a small decrease of XRD peak intensity which is the archetypal effect induced by ball-milling. The use of high energy ball milling to induce structural defects such as amorphization, microstructural refinement resulting in a loss of crystallinity of soil compounds is a well documented method [29].

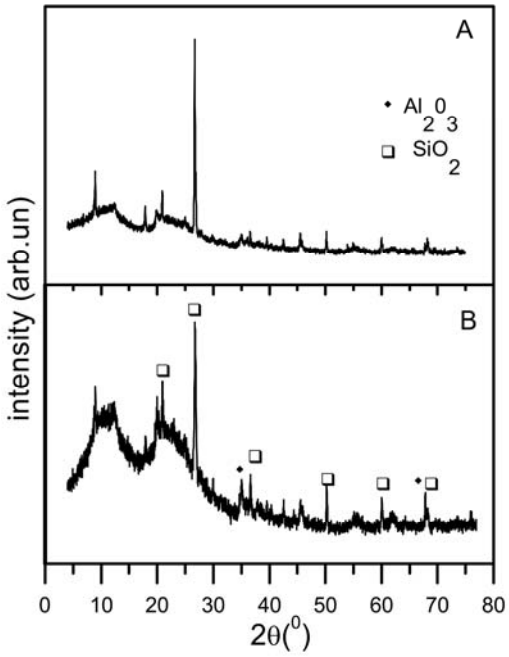

Fig.1 XRD analysis of untreated (A) and 5 hours milled (B) diatomite.

No clay minerals were found in the diatomite samples even in trace amounts since there is no any XRD peak that could be characteristic for new phases, contrary to many diatomaceous earths from other origins. The crystallite size of various species was determined using Scherer's formula. Decreasing in crystallite size of quartz and alumina when material was submitted to high energy ball milling was noticed. These modifications have a great influence on adsorption properties (see further).

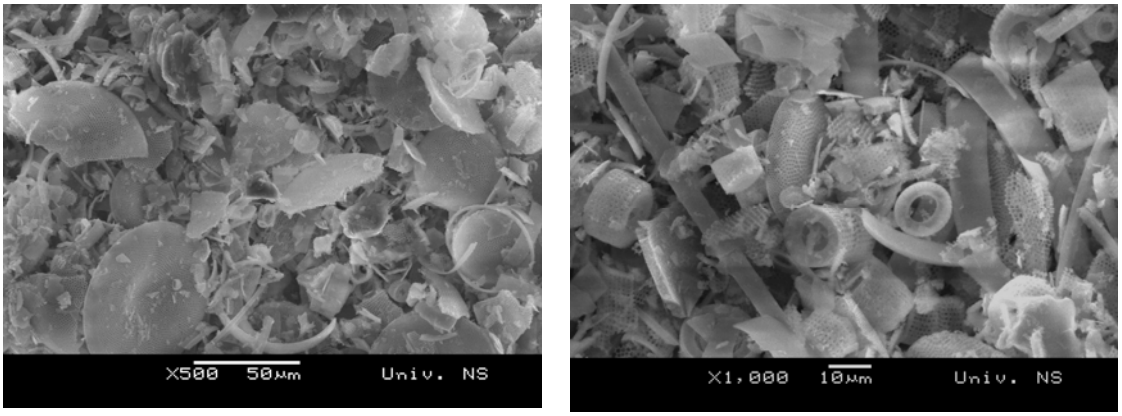

Fig.2. SEM images of untreated diatomite: (a) and mechanical treated (b)

Fig.2 represents the micrographs of raw (Fig.2a) and treated diatomite (Fig. 2b). Diatomite frustules are mainly divided into two categories; centric (discoid) and pennate (elongated to filiform). The length of the pennate shape is in the range form 10 -20 μm, while the centric diatom has a radius of approximately 20 μm. It can be noticed from the scanning micrographs that diatomite has a highly porous structure which was the main reasons to select this material as a potential sorbent for heavy metals [3] even a slight increase form 17.12m^2/g to 17.48m^2/g in specific surface area was observed during milling. As we conclude from XRD

main components of diatomite are oxides which are brittle and can be easy pulverized during mechanical milling, but one can notice from Fig. 2b, that the porous texture of diatomite is not completely damaged after ball milling. Cylindraceous diatomite (centric) particles are still present in the sample, while rod-like (pennet) particles are partially pulverized during milling.

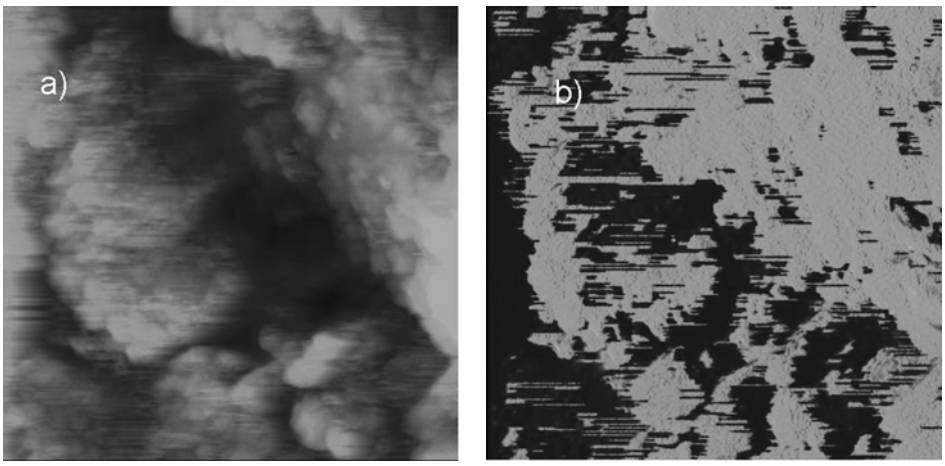

Fig.3. AFM images (5 × 5 μm) of untreated diatomite: a) topography, b) phase structure

It can be seen from the Fig 3 where the AFM micrographs of the diatomite are presented that small diatomite particles are compacted into the pellet. A sponge like structure with small pore sizes can be noticed from topography picture presented in Fig. 3a.

AFM phase analysis, presented in Fig. 3b has shown very clear differentiation of sample phase composition. Light fields can be ascribed to Si phase (according to XRD and chemical analysis SiO_2) while dark fields can be ascribed to Al (according to XRD and chemical analysis Al_2O_3) and Fe (according to chemical analysis Fe_2O_3). The hexagonal structure of the oxide unit cell is clearly visible in Fig. 4 obtained with higher magnification (400 × 400 nm). The average diameter of a single hexagon is 60 nm. These cells are close, making a terrace structure of each hexagon with randomly distributed Si and Al oxides.

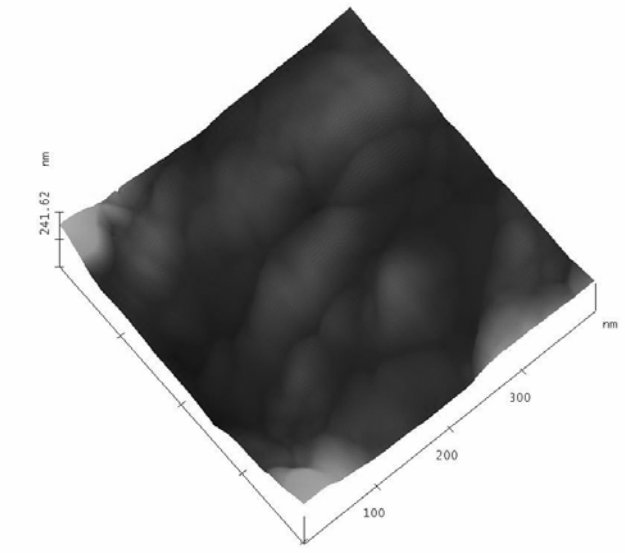

Fig.4. AFM 3D surface topography (400 × 400 nm) of untreated diatomite

AFM micrographs of ball milled diatomite samples for 5 hours are presented in the Fig. 5. One can notice that the topography of this sample has some changes in comparison. The hexagonal structure is not clearly visible anymore and the sponge-like structure is more prominent. Diatomite has become denser and compact (Fig.5a). During mechanical milling the diatomite structure has been partially destroyed and effective diameter of pore is decreased. The phase distribution has changed also. This can suggest that the real chemical composition is changed during milling. Anyhow, XRD analysis did not show new phases, so one can conclude that changes are due to amorphisation, which leads to better sorption properties of the sample.

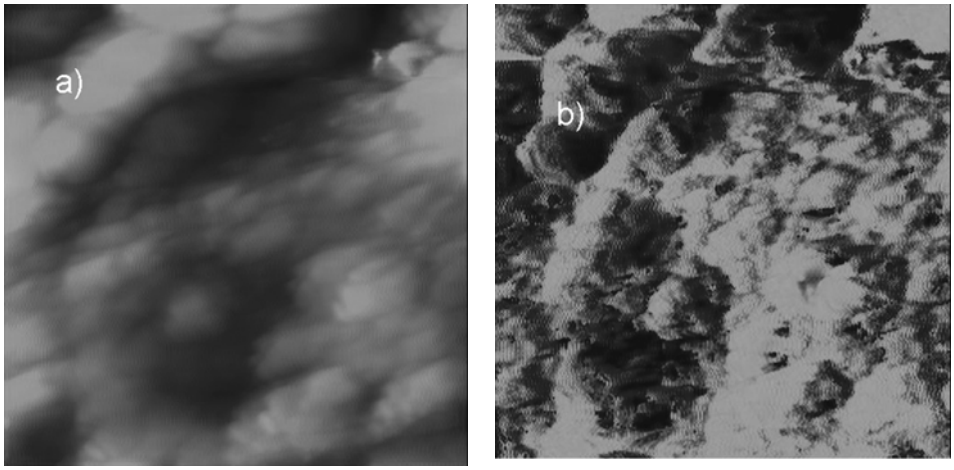

Fig.5. AFM images (2 × 2 μm) of 5 hours milled diatomite: a) topography, b) phase structure.

Comparing the topography of treated (Fig. 6) and untreated (Fig. 4) diatomite one can notice the major structural topography changes caused by milling. The hexagonal structure has disappeared and agglomerates with a sponge-like structure appear. The basic structure has been partially destroyed. Similar results are obtained with SEM analysis.

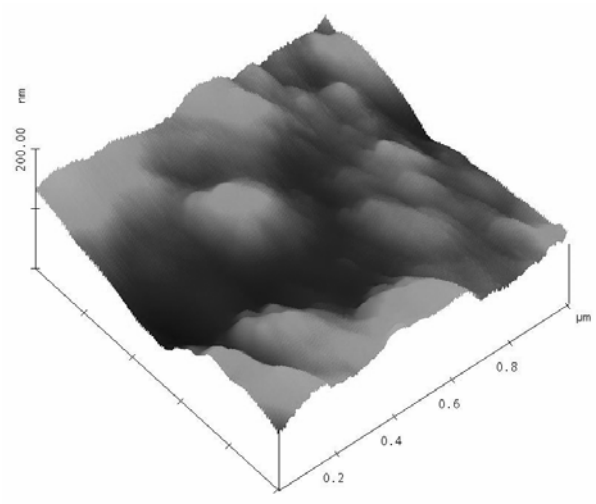

Fig. 6. AFM 3D surface topography (1μm × 1 μm) of 5 hours milled diatomite.

Concentration in the diatomite phase after 24h of immobilization versus milling time has been presented in Fig. 7. One can notice that the quantity of adsorbed Pb(II) and thus

immobilization efficiency increase when the milling time increases and achieved saturation when the milling time is 4 hours. This can be ascribed to microstructural changes emerged after ball milling, such as the appearance of a mesoporous sponge-like structure.

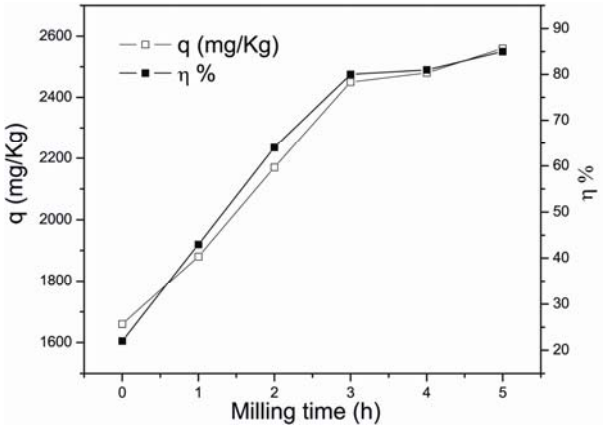

Fig.7. Pb(II) concentration in the diatomite phase after 24h (a) immobilazation efficiences of diatomite samples (b).

According to Montinaro et al [18] the best diatomite immobilization efficiency up to 97% can be achieved for the BPR (ball to powder ratio) equal to 4. Correspondingly, the concentration of Pb(II) released in the solution dramatically decreases. Our results show the immobilization efficiency raise from 22% for untreated samples to 81% to treated sample for 5h at BPR 4.

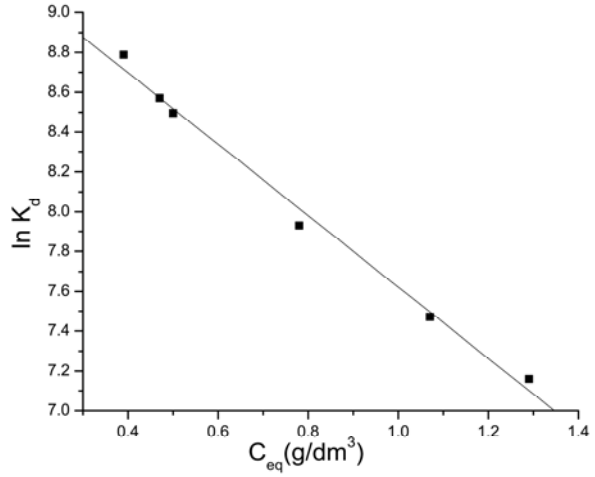

Fig. 8. Linear fit of $\ln K_d = f\left(C_{Pb(II)}^{24h}\right)$

Obtained free energy changes from linear fit of equation 3 plotted in Fig. 8 [25], and corresponding equations for ΔG^0 and ΔS^0 are ΔG^0 is -23,34 kJ/mol, while ΔS^0 = 78,3 J/mol signifying the sorption reactions are spontaneous with a high affinity.

4. Conclusion

Diatomite and modified diatomite have been tested as possible adsorbents for

removal of Pb^{2+} ions from solutions. Metal sorption capacity of diatomite is considerably improved after mechanical modification. This improvement is attributed to amorphysation of the material. Our results show that immobilization efficiency raise from 22% for untreated samples to 81% to treated sample for 5h at BPR 4.

Acknowledgement

This work is supported by the Serbian Ministry of Science and Technological development under projects 142016 and 141001.

References

1. J.F. Lemonas, Am. Ceramic Soc. Bull. 76(6) (1997) 92.
2. Y.S. Al-Degs, M.F. Tutunju, R.A.Shawabkeh, Sep. Sci. Technol. 35 (2000) 2299.
3. M.A.M. Khraisheh, Y.S. Al-Degs, W.A.M. Mcminn, Chem. Eng. J. 99 (2004) 177.
4. M. Monagheddu, G.Mulas, S. Doppiu, G. Cocco, S. Raccanelli, Environ. Sci. Technol. 33 (1999) 2485.
5. S. Martinovic, M. Vlahovic, T. Boljanac, Lj. Pavlovic, Int.Miner Process 80 (2006) 255.
6. M.A.Al-Ghouti, M.A.M.Khraisheh, S.J. Allen, J. Environ. Manage. 69 (2003) 229.
7. S.Aytas, S.Akyil, M.A.A. Aslani, U. Aytekin, J. Radioanal. Nucl. Chem. **240**(3) (1999) 973.
8. Y.X.Yang, R.S. Chen, A.B.Dai, Acta Chim. Sinica 54 (1996) 57.
9. S. Milovanovic, Lj. Matovic, M. Drvendzija, J. Grbovic Novakovic, J.Micro-Oxford, 232(3) (2008) 522.
10. H.L. Needleman, D.D. Bellinger, Annu. Rev. Public Health 12 (1991) 111.
11. E.T. Snow, Pharmacol.-Ther. 53, (1992) 31.
12. Y.M.Wang, T.C. Chen, K.J. Yeh, M.F. Shue, J. Hazard. Mater. B88, (2001) 63.
13. Majeda A.M. Khraisheh, Yahya S. Al-Degs, Wendy A.M. Mcminn, Chem. Eng. J. 99 (2004) 177.
14. Y. Orhan, H. Buyukgungor, Water Sci. Technol. 28 (1993) 247.
15. K.P. Yadava, B.S. Tyagi, V.N. Singh, J. Chem. Tech. Biotechnol. 51(1991) 47.
16. M.J. Ayotamuno, R.B. Kogbara, S.O.T. Ogaji, S.D. Probert, App. Energy 83 (2006) 1258.
17. K.K. Panday, G. Parsed, and V.N. Singh, Water Res. 19 (1985) 869.
18. S. Montinaro, A. Concas, M.Pisu, G. Cao, Chem. Eng. J. 142 (2008) 271.
19. S,Montinaro, A. Concas, M.Pisu, G. Cao, Chemosphere 67 (2007) 631.
20. W.R. Knocke and L.H. Hemphill, Water Res. 15**,** (1981) 275.
21. G. Macchi, D. Maroni, and G. Tiravarthi, Environ. Technol. Lett. 7 (1986) 431.
22. H. Farrah, D. Halton, and W.F. Puckering, Chem. Geol. 28 (1980) 55.
23. M. Šljivić, I. Smičiklas, S. Pejanović, I. Plećaš, Applied Clay Science 43(1) (2008) 33.
24. M.J. Zamazow, J.E. Murphy,. Sep. Sci. Technol. 27 (1992) 1969.
25. G. Sheng, J.Hu, X.Wang, Appl. Radiat. Isot. 66 **(**2008) 1313.
26. G.Mulas, S. Loiselle, L. Schiffini, G. Cocco,J. Solid State Chem. 129 (1997) 263.
27. Q. Zhang, H. Matsumoto, F.Saito, M. Baron, Chemosphere 48 (2002) 787.
28. S.Caschili, F. Delogu, A. Concas, M.Pisu, G. Cao,. Chemosphere 63(2006) 987.
29. C. Suryanarayana, E. Ivanov, V. Boldyrev, Mat. Sci. Eng. A 304–306 (2001) 151.

Садржај: *У овом раду проучаван је ефекат промене микростурктуре проузроковне механичким млевењем на адсорпционе особине диатомита. Микроструктуре промене праћене су рендгенском дрифракцијом, скенирајућом електронском микроскопијом и АФМ микоскопијом, док је степен адсорпције праћен атомском емисионом спектроскопијом. Резултати показују да се сорпциони капацитет диатомита значајно повећава након механичког млевења. Овај ефекат се може приписати аморфизацији материјала. Имобилизациона ефикасност материјала расте од 22% код нетретираног до 81% код третираног узорка. Повећање имобилизационе ефикасности механичким млевањем када је однос масе кугли према маси узорка (БПР) 4, а прах млевен 5 сати говори у прилог чињењици да се модификовани диатомит може користити за пречишћавање отпадних вода које садрже олово.*

Кључне речи: *Пречишћавање отпадне воде, диатомит, микроструктура, млевење, AFM.*